Inorganic Chemistry

Article

pubs.acs.org/IC

Mapping the Binding Modes of Hemilabile Pincer–Crown Ether Ligands in Solution Using Diamagnetic Anisotropic Effects on NMR Chemical Shift

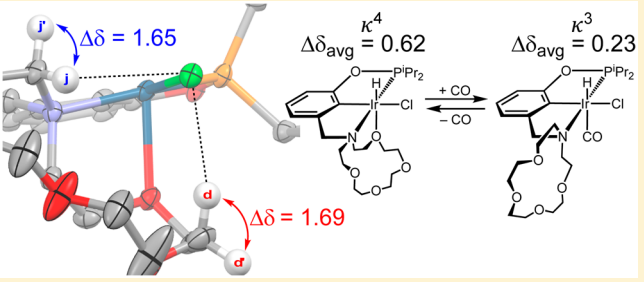
Andrew M. Camp,[†] Matthew R. Kita,[†] Javier Grajeda,[†] Peter S. White,[†] Diane A. Dickie,[‡] and Alexander J. M. Miller*[,†]

[†]Department of Chemistry, University of North Carolina at Chapel Hill, Chapel Hill, North Carolina 27599-3290, United States

[‡]Department of Chemistry, Brandeis University, 415 South Street, Waltham, Massachusetts 02453, United States

Supporting Information

ABSTRACT: A protocol for identifying ligand binding modes in a series of iridium pincer complexes bearing hemilabile aza-crown ether ligands has been developed using readily accessible NMR methods. The approach was tested on a collection of 13 structurally diverse pincer–crown ether complexes that include several newly characterized species. New synthetic routes enable facile interconversion of coordination modes and supporting ligands. Detailed structural assignments of five complexes reveal that the difference in chemical shift ($\Delta\delta$) between geminal protons in the crown ether is influenced by diamagnetic anisotropy arising from halides and other ligands in the primary coordination sphere. The average difference in chemical shift between diastereotopic geminal protons in the crown ether macrocycle ($\Delta\delta_{avg}$), as determined through a single $^{1}H-^{13}C$ HSQC experiment, provides information on the pincer ligand binding mode by establishing whether the macrocycle is in close proximity to the metal center. The $\Delta\delta_{avg}$ values for binding modes that involve chelating ether(s) bound to iridium are roughly 2-fold larger than those for tridentate complexes with no Ir–O bonds.



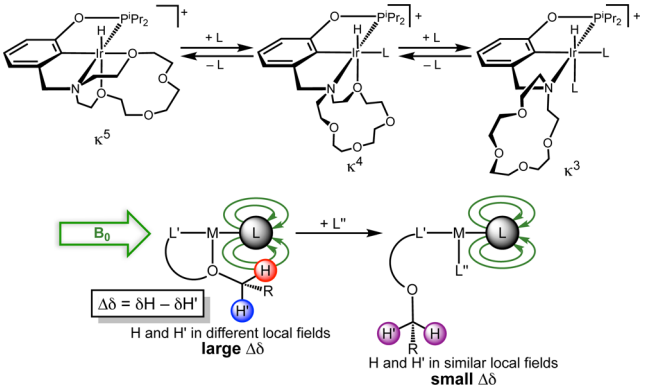
INTRODUCTION

Hemilabile ligands have emerged as broad and versatile tools in coordination chemistry.[1] As chelates with a weak donor that can dissociate or be displaced from the metal center, hemilabile ligands balance the stability of coordinatively saturated metal complexes with the activity provided by facile ligand substitution at the weak donor site. This balance has been particularly fruitful in the preparation of catalysts with high activity and good stability[2−4] as well as catalysts that can be recycled through control of the hemilabile ligand binding mode.[5,6]

In pursuit of catalysts that can be tuned using cationic additives, we have developed "pincer–crown ether" ligands that contain an aza-crown ether macrocycle capable of multiple hemilabile coordination modes.[7−9] As shown in Scheme 1, pincer–crown ether ligands can adopt a tridentate (κ^3) binding mode like that of traditional pincer ligands, or weak ether donors can bind to reach tetradentate (κ^4) or pentadentate (κ^5) binding modes.[10]

It can be challenging to characterize the different binding modes of hemilabile ligands in solution. The weak donors can bind to the metal center, dissociate to form a low-coordinate species, or be displaced by solvent or another external donor ligand. In some cases, the binding modes interconvert rapidly ("dynamic hemilability"), while in other cases isomerization can be slow or require a chemical impetus ("static hemilability").[7,11] Crystallographic characterization can readily identify binding modes in the solid state.[7,12] It is more difficult to probe the binding mode of a hemilabile ligand in solution.

Scheme 1. Pincer–Crown Ether Ligand Binding Modes and Effect of Diamagnetic Anisotropy on Proximal Protons



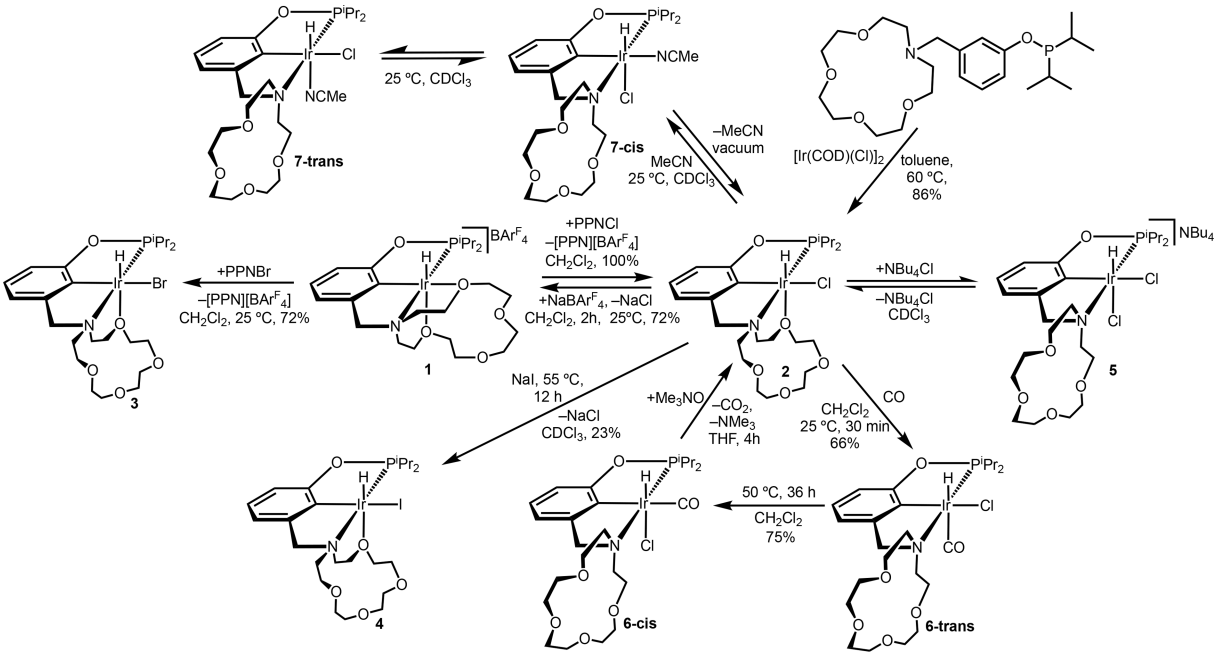
Received: June 10, 2017
Published: September 5, 2017

Downloaded via LBRY FOR NATURAL SCIENCES RAS on August 23, 2018 at 07:39:41 (UTC).
See https://pubs.acs.org/sharingguidelines for options on how to legitimately share published articles.

© 2017 American Chemical Society

DOI: 10.1021/acs.inorgchem.7b01485
Inorg. Chem. 2017, 56, 11141−11150

Scheme 2. Synthetic Access to Pincer–Crown Ether Complexes in Various Coordination Modes



In this work, a collection of well-defined pincer–crown ether complexes has been used to develop a new NMR protocol for identifying the coordination mode of these hemilabile ligands in solution. The protocol connects the hemilabile ligand coordination mode to chemical shift differences based on the presence of diamagnetic anisotropy induced by other ligands at the metal center. Diamagnetic anisotropy influences chemical shifts through the field-induced movement of paired electrons, which generates local secondary fields.[13] This differs from paramagnetic anisotropy, which influences chemical shifts over hundreds of parts per million (ppm) through field-induced movement of unpaired electrons.[14] Diamagnetic anisotropic effects from organic arenes,[15] carbonyls,[16] and nitriles[17] have been shown to significantly influence chemical shifts, thus providing valuable structural information on complex organic molecules and proteins in solution.[14,18,19] While not used routinely in inorganic systems, diamagnetic anisotropy has been productively applied to structural determination of ruthenium(II) diastereomers,[20] characterization of metal–metal quadruple bonds,[21] and the orientation of complexes of the type (arene)M(CO)$_3$.[22,23]

In pincer–crown ether ligands, the chemical shifts of geminal protons in the crown are sensitive to the proximity of the macrocycle to other ligands bound to the metal. The difference in chemical shift between geminal protons ($\Delta\delta$) can serve as a marker of the coordination mode (Scheme 1). Focusing on pincer–crown ether complexes as a convenient development platform, a protocol for gaining insight into hemilabile ligand coordination mode is developed on the basis of a concise series of routine and inexpensive NMR experiments.

RESULTS AND DISCUSSION

Synthetic Access to Different Binding Modes. *Synthesis and Characterization of Halide-Containing Pincer–Crown Ether Complexes.* Synthetic routes to a large array of pincer–crown ether complexes with different coordination modes of the pincer–crown ether ligand are shown in Scheme 2. As discussed in the following paragraphs, complexes **3**, **4**, **5**, and **6-trans** have not been previously characterized. The ligand coordination modes of several complexes have been assigned on the basis of solid-state crystallographic studies. NMR spectroscopic studies suggest that the coordination mode is maintained in solution for noncoordinating solvents such as chloroform and dichloromethane, as detailed below.

The previously reported iridium hydride [κ^5-(^{15c5}NCOP^{iPr})Ir(H)][BAr$^F_4$] (**1**) adopts a pentadentate binding mode, with two crown ether oxygen atoms binding the metal center, both in the solid state and in noncoordinating, chlorinated solvents.[7] Hydride resonances in ^{1}H NMR spectra provide a convenient marker of solution-phase structure. The ligand trans to the hydride has a big impact on the chemical shift of the hydride resonance.[24] The hydride in **1** has a ^{1}H NMR chemical shift (δ −30.03) in $CDCl_3$ that is indicative of an ether donor trans to the hydride.[25]

The pentadentate-bound complex **1** serves as a convenient starting place for examining changes in binding mode, as the weak ether donors can undergo ligand substitution reactions. Addition of 1 equiv of PPNCl (PPN = bis(triphenylphosphine)iminium) to cationic hydride complex **1** in CH_2Cl_2 (Scheme 2) has been shown to yield the tetradentate-bound chloride complex κ^4-(^{15c5}NCOP^{iPr})Ir(H)(Cl) (**2**) featuring one ether bound to Ir.[26] Complex **2** can also be accessed by metalation of the pincer ligand with [Ir(COD)(Cl)]$_2$.[7] A crystallographic study previously established that the pincer ligand in **2** adopts a tetradentate binding mode in the solid state.[7] In $CDCl_3$ solution, compound **2** is characterized by a hydride resonance (δ −31.26) consistent with the weak ether donor remaining in the site trans to the hydride. The chloride can be abstracted from **2** with 1 equiv of NaBAr$^F_4$ to reform **1** (Scheme 2).[7]

Tetradentate-bound complexes of other halides were also targeted. Addition of PPNBr to a solution of **1** in CH_2Cl_2 at room temperature yields a new bromide complex, κ^4-(^{15c5}NCOP^{iPr})Ir(H)(Br) (**3**), in 72% yield (Scheme 2). Successful incorporation of bromide was confirmed by high-resolution mass spectrometry (HRMS). The hydride resonance

DOI: 10.1021/acs.inorgchem.7b01485
Inorg. Chem. 2017, 56, 11141–11150

(δ −31.23) is consistent with a tetradentate pincer coordination mode with the ether donor trans to the hydride.

The analogous iodide complex was prepared in a different manner, via halide exchange in **2**. Heating a solution from **2** in $CDCl_3$ in the presence of excess NaI yields κ^4-(^{15c5}NCOP^{iPr})-Ir(H)(I) (**4**) (Scheme 2), as confirmed by HRMS studies. The hydride resonance (δ −31.20) has a chemical shift that is almost identical to that of **3**, suggesting an analogous tetradentate structure in solution.

Complexes with a meridional tridentate binding mode of the pincer ligand are accessible from the hydridochloride **2**. Sequential addition of portions of NBu_4Cl to **2** leads to a new species identified as the anionic dichloride κ^3-[(^{15c5}NCOP^{iPr})Ir(H)$(Cl)_2$]$^-$ (**5**) (Scheme 2). The growth of a new hydride peak downfield of **2** (δ −24.4) suggests that chloride has displaced the ether ligand. More than 150 equiv of NBu_4Cl was required to reach 99% conversion, precluding isolation of **5**.

Binding of CO was then investigated. When a pale-yellow solution of **2** in CH_2Cl_2 is placed under 1 atm CO at room temperature, the color immediately fades. Two products, observed in a 15:1 ratio, are assigned as *trans*-κ^3-(^{15c5}NCOP^{iPr})-Ir(H)(Cl)(CO) (**6-trans**) and *cis*-κ^3-(^{15c5}NCOP^{iPr})Ir(H)(CO)-(Cl) (**6-cis**) (Scheme 2). The major species, **6-trans**, features a hydride resonance characteristic of a carbonyl trans to the hydride (δ −7.02; cf. the hydride resonance of **6-cis** at δ −19.22). In the ^{13}C NMR spectrum of **6-trans**, the carbonyl carbon appears as a doublet of doublets (δ 178.88, $^2J_{HC}$ = 56.6 Hz, $^2J_{PC}$ = 3.4 Hz) with the strong carbon−proton coupling expected in a *trans*-hydridocarbonyl geometry. Isomer **6-cis** shows only coupling attributed to phosphorus (δ 180.76, $^2J_{PC}$ = 4.6 Hz). Single crystals of **6-trans** suitable for an X-ray diffraction (XRD) study grew after pentane was layered over a concentrated solution of **6-trans** in toluene. The solid-state structure of **6-trans** (Figure 1A) features no crown ether oxygen interactions with the iridium center, confirming a tridentate binding mode of the pincer ligand.

The coordination isomer **6-cis**, with the carbonyl cis to the hydride, was previously characterized (including an XRD study confirming the expected κ^3 binding mode) as the sole product of metalation of the free pincer−crown ether ligand with Ir$(CO)_2$(Cl)(*p*-toluidine) in refluxing toluene.[8] Hypothesizing that **6-trans** was the kinetic product of ether displacement from **2**, the 15:1 **6-trans**/**6-cis** mixture was heated at 50 °C for 36 h. Thermal redistribution of the isomers resulted in a 1:3 ratio favoring the **6-cis** isomer. Heating isolated samples of pure **6-cis** did not produce detectable levels of **6-trans**, suggesting that **6-cis** is the thermodynamic product. This is consistent with prior reports of iridium hydridocarbonyl chloride complexes.[27−29]

The carbonyl ligands of **6-trans** and **6-cis** are stable under prolonged exposure to dynamic vacuum at room temperature. However, the carbonyl ligand of **6-cis** can be removed using trimethylamine *N*-oxide, a decarbonylation reagent that has been successfully applied to other systems.[30] Stirring **6-cis** and Me_3NO in THF for 48 h provides a new route to move between coordination modes, generating **2** as the only hydride-containing species according to ^{1}H NMR spectroscopy. The expected trimethylamine byproduct was present as a singlet at δ 2.11 (Scheme 2).

Acetonitrile has been previously shown to bind to hydridochloride **2**, producing an equilibrium mixture comprising the starting material **2** and the two coordination isomers

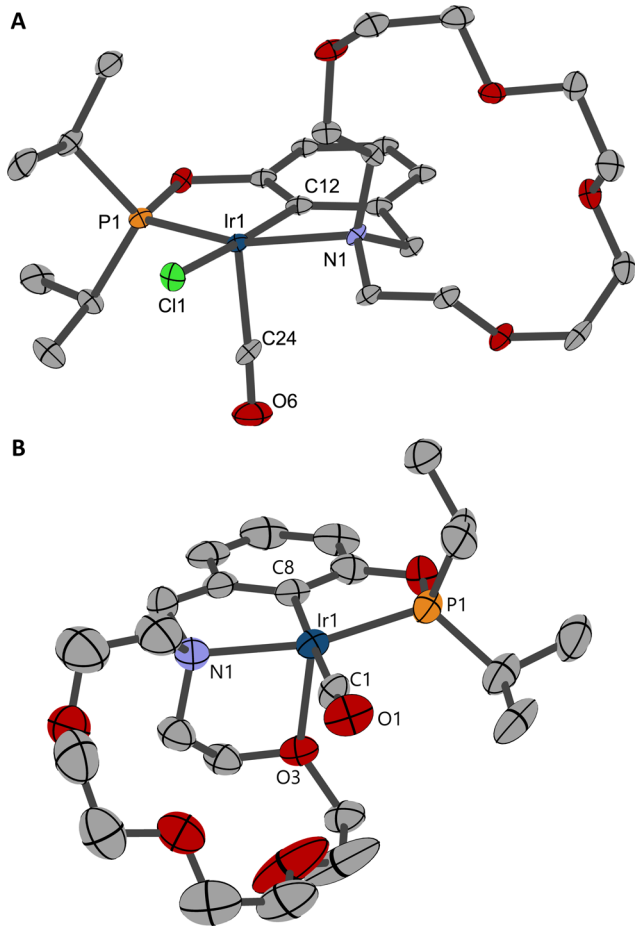


Figure 1. Structural representations of **6-trans** (A) and one of the two independent cations of **8** in the asymmetric unit (B), with ellipsoids drawn at the 50% probability level. Hydrogen atoms and counterions have been omitted for clarity. A 14% substitutional disorder of CO and Cl ligands was observed for **6-trans**, consistent with some cocrystallized **6-cis**; further information on refinement is available in the Supporting Information.

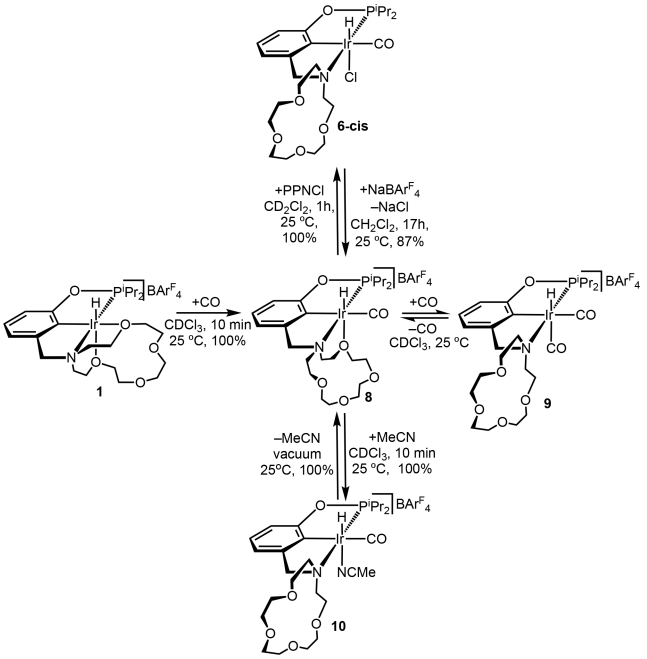
trans-κ^3-(^{15c5}NCOP^{iPr})Ir(H)(Cl)$(NCCH_3)$ (**7-trans**) and *cis*-κ^3-(^{15c5}NCOP^{iPr})Ir(H)$(NCCH_3)$(Cl) (**7-cis**). Applying dynamic vacuum to the mixture at room temperature regenerates **2** (Scheme 2).[7]

Synthesis and Characterization of Carbonyl-Containing Pincer−Crown Ether Complexes. A larger array of carbonyl complexes could be accessed conveniently from pentadentate-bound **1**, as shown in Scheme 3. Placing **1** under 1 atm CO in $CDCl_3$ leads to a mixture of two products at room temperature. The minor product is assigned as the new cationic hydridocarbonyl [κ^4-(^{15c5}NCOP^{iPr})Ir(H)(CO)][$BAr^F{}_4$] (**8**), which exhibits a tetradentate binding mode with an ether donor trans to the hydride (δ −25.79). The major product is assigned as the new dicarbonyl complex [κ^3-(^{15c5}NCOP^{iPr})Ir-(H)$(CO)_2$][$BAr^F{}_4$] (**9**) on the basis of the downfield hydride resonance at δ −9.43, which is indicative of a strong donor trans to the hydride.

Exposing the mixture of **8** and **9** to dynamic vacuum at room temperature yields **8** as the exclusive product. Crystals of **8** suitable for an X-ray diffraction study were grown by slow evaporation of an Et_2O solution. Figure 1B shows that **8** adopts a tetradentate binding mode in the solid state, with a crown ether oxygen donor trans to the hydride.

DOI: 10.1021/acs.inorgchem.7b01485
Inorg. Chem. 2017, 56, 11141−11150

Scheme 3. Synthetic Access to a Family of Carbonyl-Containing Pincer–Crown Ether Complexes



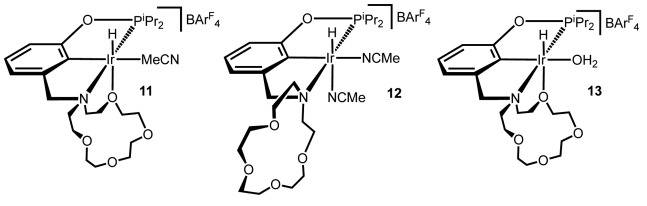
A mixed ligand system with a tridentate binding mode is accessible by addition of excess acetonitrile to **8** in $CDCl_3$ to yield $[\kappa^3\text{-}(^{15c5}NCOP^{iPr})Ir(H)(CO)(NCCH_3)][BAr^F{}_4]$ (**10**).[8] The hydride peak shifts to an intermediate range (δ −19.83) when acetonitrile displaces the ether donor. The acetonitrile ligand can be removed under dynamic vacuum to regenerate the tetradentate hydridocarbonyl complex **8**.

Addition of 1 equiv of PPNCl to monocarbonyl **8** in CH_2Cl_2 leads to the hydridocarbonyl chloride complex **6-cis** after 1 h (NMR spectroscopy). This reaction offers yet another route to complex **6-cis**; the same species can also be accessed by addition of CO to hydridochloride **2** followed by thermolysis (see above) or by direct metalation of the free ligand with a carbonyl precursor.[8] Abstracting the chloride from **6-cis** with 1 equiv of $NaBAr^F{}_4$ in CH_2Cl_2 generates **8** (Scheme 3).

Summary of Iridium Pincer–Crown Ether Substitution Reactions. Many iridium pincer–crown ether species are accessible by several different synthetic routes, and almost every reaction can be reversed by applying a vacuum or through a chemical reaction. Ligands beyond halides and carbon monoxide have also been explored and are included for the NMR studies that follow.

The complexes in Chart 1 have been previously prepared by addition of a ligand to complex **1**. The tetradentate-bound acetonitrile complex $[\kappa^4\text{-}(^{15c5}NCOP^{iPr})Ir(H)(NCCH_3)][BAr^F{}_4]$ (**11**) and the tridentate-bound bis(acetonitrile) complex $[\kappa^3\text{-}(^{15c5}NCOP^{iPr})Ir(H)(NCCH_3)_2][BAr^F{}_4]$ (**12**) can be prepared using different amounts of acetonitrile.[7] Water can also bind to **1** to generate another tetradentate-bound species, $[\kappa^4\text{-}(^{15c5}NCOP^{iPr})Ir(H)(H_2O)][BAr^F{}_4]$ (**13**).[7]

Chart 1



The wide variety of pincer–crown ether coordination modes and the range of available exogenous ligands make this system ideal for NMR studies probing hemilabile ligand binding modes.

NMR Methods for Identifying Pincer–Crown Ether Coordination Modes. In hopes of identifying a simple NMR protocol for distinguishing between different hemilabile ligand coordination modes, we first performed a full assignment on just a few selected pincer–crown ether complexes. Routine characterization always involves the acquisition of ^1H, $^{31}P\{^1H\}$, and $^{13}C\{^1H\}$ NMR spectra. Full proton assignments for **1**, **2**, **3**, **6**, and **8** were made using a combination of multidimensional experiments, including $^1H-^{13}C$ HSQC, $^1H-^{13}C$ HSQC-TOCSY, $^1H-^1H$ COSY, and $^1H-^{13}C$ HMBC. Complete spectral details and assignments are provided in the Supporting Information.

The ^1H NMR spectrum of the free ligand is shown in Figure 2A. The labeling scheme for all of the complexes is shown in Figure 2A; carbon atoms are labeled with uppercase letters, and hydrogen atoms are given lowercase letters (e.g., C_A and H_a/$H_{a'}$). The crown ether region of the free ligand is crowded with 16 overlapping proton resonances centered at δ 3.63 and a triplet at δ 2.76 (4H integration). The upfield resonance is characteristic of a pair of equivalent methylene groups adjacent to nitrogen.[31]

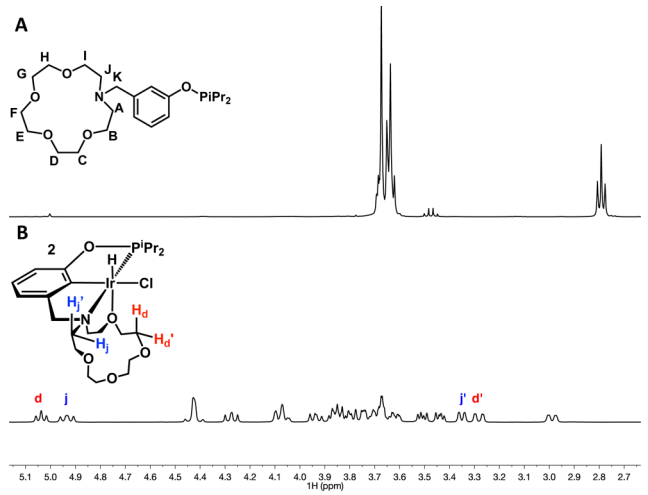


Figure 2. Comparison of the ^1H NMR spectra (crown ether region) of the free ligand (A) and **2** (B). Atom labels are consistent across all of the complexes.

The chloride complex **2** features a well-resolved ^1H NMR spectrum with resonances spanning a wide range (Figure 2B). Nuclear Overhauser effect spectroscopy (NOESY) studies confirmed that a tetradentate coordination mode is maintained in solution (Figure 3). Through-space coupling between the isopropyl methyl protons and crown ether protons indicates that the macrocycle adopts a conformation that places methylene protons near the metal center. Such NOE interactions have not been observed in the free ligand or in complexes that adopt a tridentate coordination mode.

Complex **2** features two crown ether protons that are shifted dramatically downfield (H_d and H_j; Figure 2B). Downfield shifts have been observed in chelating ethers in Ir complexes,[32]

DOI: 10.1021/acs.inorgchem.7b01485
Inorg. Chem. 2017, 56, 11141–11150

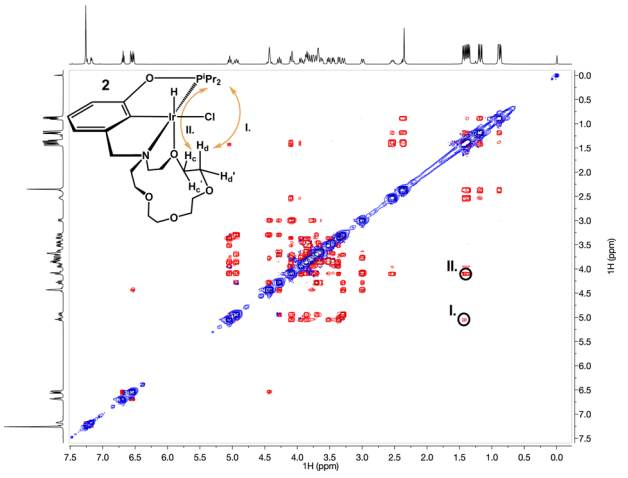


Figure 3. ^{1}H−^{1}H NOESY spectrum of **2**. Cross-peaks between methyl protons of the isopropyl group and H_d (I) and H_c (II) support a tetradentate binding mode.

so it would be reasonable to assign these resonances as the protons closest to the metal center. However, multinuclear, two-dimensional NMR analysis revealed that the most downfield crown ether resonances correspond to two protons that are *not* adjacent to the metal center—they are in fact *far apart* in the macrocycle.

Comparisons with crystallographic data show that downfield protons H_d and H_j in **2** are in close proximity to the chloride ligand in the solid-state structure. As shown in Figure 4, the

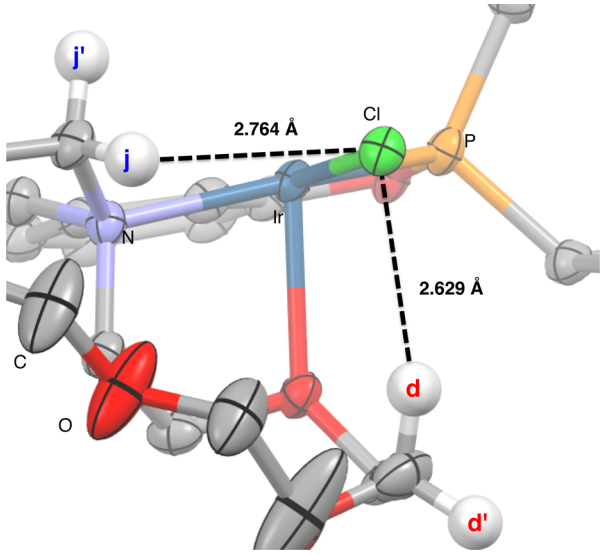


Figure 4. Molecular representation of **2** (from X-ray crystallographic data)[7] showing the proximity of protons H_j and H_d to the chloride ligand.

Cl−H_d and Cl−H_j distances are 2.629 and 2.764 Å, respectively. On the other hand, the other protons of these geminal pairs ($H_{d'}$ and $H_{j'}$) are oriented away from the group in space. The resonances for $H_{d'}$ and $H_{j'}$ are found in the typical region for ethers, leading to chemical shift differences between the diastereotopic geminal protons ($\Delta\delta$) of 1.69 ppm ($\Delta\delta_{d/d'}$) and 1.65 ppm ($\Delta\delta_{j/j'}$). The data suggest that chloride anisotropy is responsible for the large downfield shifts for H_d and H_j in **2** (δ 5.04 and δ 4.93, respectively, in Figure 2B) and the large $\Delta\delta$ values for the geminal pairs.

If the downfield resonances of **2** are due to diamagnetic anisotropy of the chlorine lone pairs, larger halogens should have a more dramatic effect on the chemical shifts.[33] In the analogous bromide complex κ^4-(^{15c5}NCOP^{iPr})Ir(H)(Br) (**3**), the same protons H_d and H_j are further deshielded to δ 5.05 and δ 5.11, respectively. The differences in chemical shift between the two geminal protons increase as well ($\Delta\delta_{d/d'}$ = 1.72 ppm and $\Delta\delta_{j/j'}$ = 1.84 ppm). Similarly, the iodide complex κ^4-(^{15c5}NCOP^{iPr})Ir(H)(I) (**4**) features downfield crown ether resonances at δ 5.29 and δ 5.04 and even larger differences in chemical shift for the diastereotopic protons ($\Delta\delta_{d/d'}$ = 1.79 ppm and $\Delta\delta_{j/j'}$ = 2.06 ppm).

The NMR spectra of the halide complexes suggest that anisotropic effects from the halide ligands induce the observed downfield shifts and large $\Delta\delta$ values when the ligand adopts a coordination mode that brings the macrocycle close to the transition metal center. It is worth noting that steric interactions could potentially give rise to similar shifts, although these are usually observed only in extremely rigid systems.[34−36]

Hydridocarbonyl chloride **6-cis** features a tridentate coordination mode in which the macrocycle has no ligated ethers. Only the eight ethylene linker protons proximal to the nitrogen show distinct chemical shifts in **6-cis**, while the rest of the crown ether protons are observed as a multiplet at δ 3.6−3.7 (Figure 5A). The largest $\Delta\delta$ value is only 0.55 ppm,

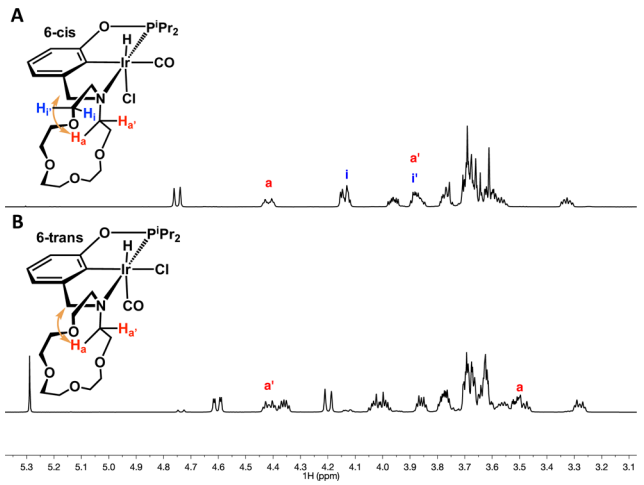


Figure 5. Comparison of the ^{1}H NMR spectra of complexes **6-cis** (A) and **6-trans** (B). Key protons were assigned on the basis of NOESY interactions with the benzylic linker (orange arrows).

corresponding to a pair of protons $H_{a/a'}$ adjacent to the amine nitrogen. Proton H_a in **6-cis** (δ 4.44) is 2.779 Å from the chloride in the X-ray diffraction structure and is deshielded relative to its partner $H_{a'}$ (δ 3.89) (Figure 6A).[8]

The geometric isomer **6-trans** also shows the largest $\Delta\delta$ values for the methylene unit adjacent to the amine nitrogen. In **6-trans**, however, it is $H_{a'}$ that is now oriented toward the chloride (2.740 Å; Figure 6B), leading to a downfield shift for $H_{a'}$ (δ 4.41). H_a is oriented away from the chloride in **6-trans** and has the more upfield shift (δ 3.51; Figure 5B). This isomer-dependent change illustrates how proximity to the chloride ligand gives rise to anisotropy-induced changes in chemical shift.

DOI: 10.1021/acs.inorgchem.7b01485
Inorg. Chem. 2017, 56, 11141−11150

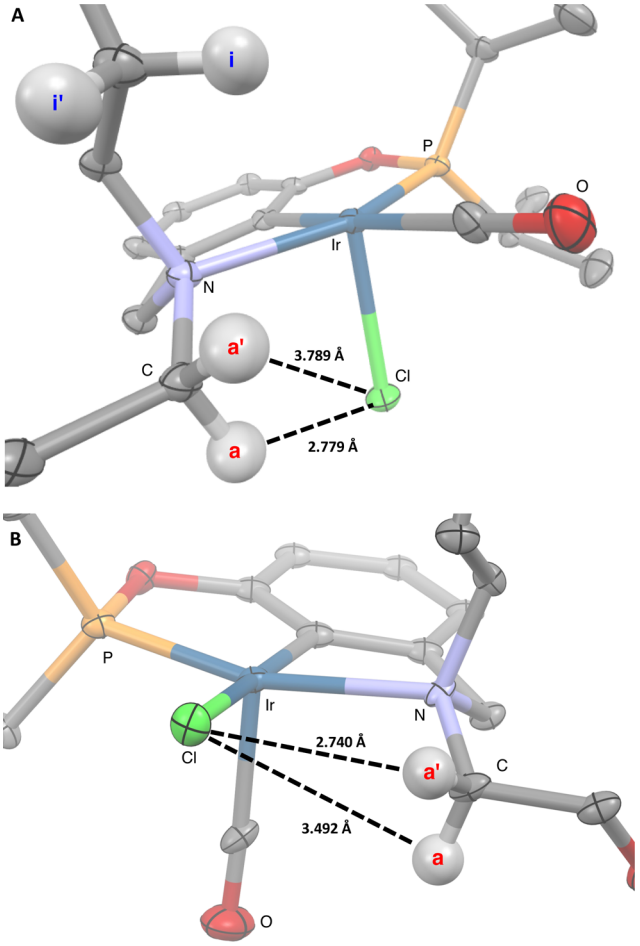


Figure 6. Molecular representation of **6-cis** (from X-ray crystallographic data),[8] showing the proximity of proton H_a to the chloride ligand (A). Molecular representation of **6-trans** (from X-ray crystallographic data), showing that proton $H_{a'}$ is proximal to the chloride ligand (B).

Tridentate-bound complexes experience less chloride-induced anisotropy overall: anisotropic shifting is limited to the methylene units closest to the amine (and closest to the metal center). This suggests that $\Delta\delta$ values are markers of hemilabile ligand coordination modes.

To determine whether $\Delta\delta$ could be applied in halide-free cases, pentadentate-bound cation **1** and tetradentate-bound carbonyl cation **8** were fully assigned. As shown in Figure 7A, the largest chemical shift difference between geminal protons in **1** is observed for $H_{j/j'}$ (δ 4.20 and δ 3.37, $\Delta\delta$ = 0.83 ppm), followed by $H_{d/d'}$ ($\Delta\delta$ = 0.55 ppm). The significant $\Delta\delta$ values may originate from oxygen diamagnetic anisotropy from the ethers in the crown,[37,38] from steric congestion,[35] or from constraint of the methylene groups.[39]

One large $\Delta\delta$ of 1.27 ppm is seen in **8**, consistent with the rigid conformation of the tetradentate coordination mode bringing crown protons close to the ligand (Figure 7B). The other diastereotopic protons show low-to-moderate $\Delta\delta$, ranging from 0.01 to 0.57 ppm. In general, the $\Delta\delta$ values are lower for halide-free systems, indicating weaker anisotropic effects from the bound carbonyl ligand.[22] However, the tridentate bis(carbonyl) **9** still has smaller chemical shift differences than the tetradentate and pentadentate analogues. Most of the geminal pairs have $\Delta\delta$ less than 0.1 ppm; the largest $\Delta\delta$ value of 0.37 ppm is assigned to the protons nearest to nitrogen. Taken together, these examples show that $\Delta\delta$ values are sensitive to the pincer−crown ether ligand binding mode.

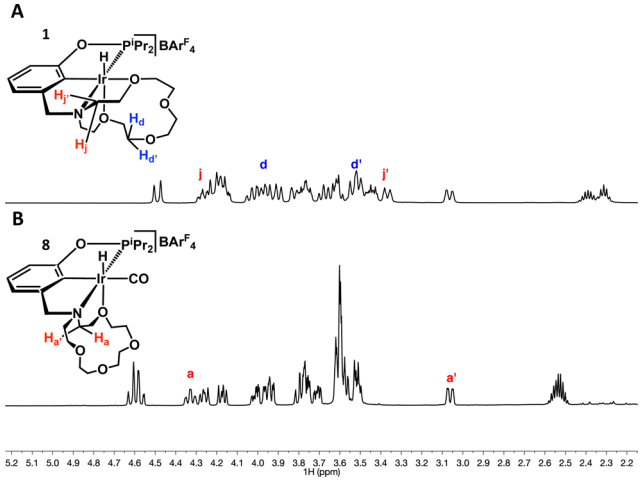


Figure 7. ^{1}H NMR spectra (crown ether region) of **1** (A) and **8** (B).

Average Differences in Chemical Shift ($\Delta\delta_{avg}$) of Geminal Protons as a Marker of Pincer−Crown Ether Coordination Mode. The full family of complexes was evaluated by ^{1}H NMR spectroscopy along with ^{1}H−^{13}C HSQC and ^{1}H−^{1}H COSY experiments. The HSQC experiment identifies which protons are attached to the same carbon, allowing facile measurement of $\Delta\delta$ values for each geminal pair in the crown ether macrocycle, while the ^{1}H NMR and COSY data assist with calculation of $\Delta\delta$ values in cases where HSQC cross-peaks are not resolved. The values of $\Delta\delta$ for the individual geminal pairs in the macrocycle were averaged to give $\Delta\delta_{avg}$. Each value of $\Delta\delta$ has some uncertainty stemming from the ability to resolve the protons in the NMR experiments. In general, the 2D experiments provide resolution of about 0.01 ppm, but when many protons have similar chemical shifts (more common in the tridentate binding mode), there is more uncertainty in each $\Delta\delta$ value and thus in the composite value of $\Delta\delta_{avg}$. Details of which experiments were performed on each complex and explanations of uncertainty can be found in the Supporting Information.

The power of this method lies in its ability to provide a useful metric of the coordination mode (the value of $\Delta\delta_{avg}$) without requiring full structural assignment of all protons in the system; only a ^{1}H NMR spectrum and ^{1}H−^{13}C HSQC and ^{1}H−^{1}H COSY experiments are needed. For example, samples of complex **9** contain small amounts of **8** (see above); this prevents full assignment of each proton in **9**, but $\Delta\delta$ values can still be readily extracted (Figure S88). The value of $\Delta\delta_{avg}$ is sensitive to large $\Delta\delta$ values, but because $\Delta\delta_{avg}$ weights each crown proton equally, macrocycles with little variation in the chemical shift of diastereotopic pairs will shift the average toward smaller values.

The $\Delta\delta_{avg}$ values for 13 complexes are collected in Figure 8. A significant difference in $\Delta\delta_{avg}$ is apparent when comparing complexes assigned to tridentate and tetradentate binding modes. In halogen-free examples, tetradentate and pentadentate species have $\Delta\delta_{avg}$ values around 0.34, more than double that of tridentate species ($\Delta\delta_{avg} \approx 0.12$). This effect is amplified in chloride-containing species, resulting in an approximately 4-fold difference in $\Delta\delta_{avg}$ between coordination modes. This protocol

DOI: 10.1021/acs.inorgchem.7b01485
Inorg. Chem. 2017, 56, 11141−11150

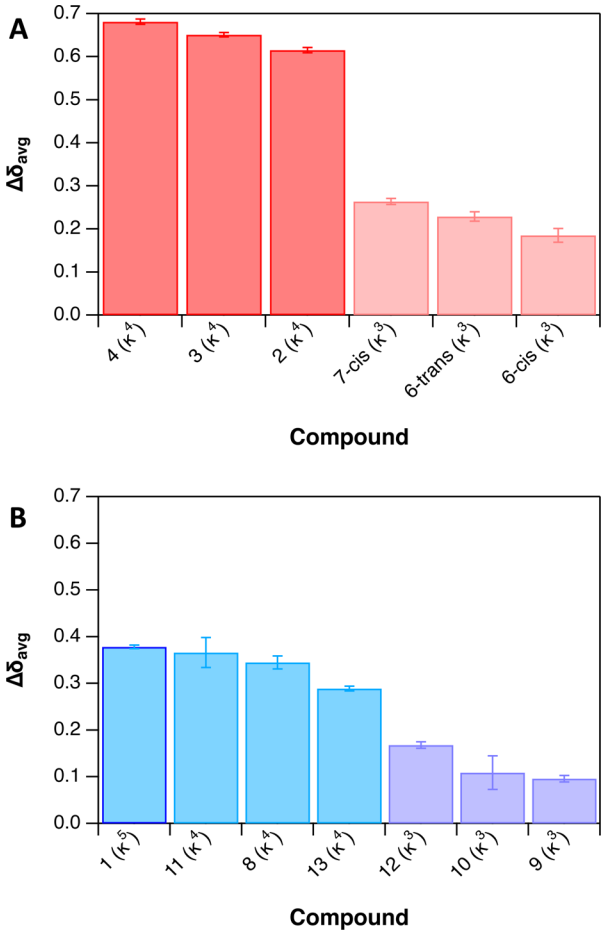


Figure 8. Bar graphs showing the average difference in chemical shift ($\Delta\delta_{avg}$) for geminal protons in the macrocycles of halide-containing (A) and halide-free (B) pincer crown ether complexes. Tetradentate- and pentadentate-bound complexes are shown in dark red (A) or blue (B), while tridentate-bound complexes are shown in light pink (A) or purple (B).

readily distinguishes between hemilabile ligand binding modes of pincer−crown ethers using a relatively concise number of NMR experiments.

CONCLUSIONS

Facile synthetic access to a structurally diverse series of iridium pincer−crown ether complexes has enabled the development of an NMR protocol that reports the presence of iridium−oxygen interactions of these hemilabile ligands in solution. Assignment of each crown ether proton of a few complexes and comparison to solid-state structures revealed that diamagnetic anisotropy dramatically influences the chemical shift in the tetradentate and pentadentate coordination modes, which bring the macrocycle close to the metal center through ether donation to iridium. A parameter based on the difference in chemical shift between diastereotopic methylene protons, $\Delta\delta_{avg}$, was found to be sensitive to the pincer−crown ether ligand binding mode. Tetradentate and pentadentate binding modes that feature ether(s) binding iridium have more than 2-fold larger $\Delta\delta_{avg}$ values compared with tridentate examples that lack Ir−O bonds.

The pincer−crown ether complexes feature hemilabile oxygen donor ligands, as is common in other hemilabile ligands,[2,3,40−42] and the metal coordination sphere is completed by commonly encountered ligands such as halides, carbon monoxide, and acetonitrile. Many hemilabile ligands feature methylene linkers that would be suitable for obtaining $\Delta\delta$ values when the protons are diastereotopic.[32,43−46] Thus, it is possible that future studies might find diamagnetic anisotropy to be a helpful probe of the coordination chemistry of hemilabile ligands beyond pincer−crown ether systems. Every system will be different, of course, but the present example shows that the meaning of $\Delta\delta$ in a particular system can be made clear through full assignments of a few key complexes, followed by rapid collection of $^{1}H-^{13}C$ HSQC data for a wider range of complexes.

EXPERIMENTAL SECTION

General Considerations. Air- and moisture-free reactions were performed using a vacuum line, Schlenk techniques, or in a glovebox under nitrogen. Under standard glovebox operating conditions, pentane, diethyl ether, benzene, toluene, and tetrahydrofuran were used without purging, such that traces of these solvents were present in the atmosphere and in solvent bottles. NMR samples were prepared in Teflon-sealed NMR tubes under a nitrogen atmosphere in the glovebox. A purge was performed prior to sample preparation to minimize solvent impurities in NMR spectra. NMR solvents were purchased from Cambridge Isotope Laboratories. Benzene-d_6 (C_6D_6), chloroform-d with tetramethylsilane (0.03%) ($CDCl_3$ w/TMS), and dichloromethane-d_2 (CD_2Cl_2) were freeze−pump−thawed three times for degassing and dried by passage through a small plug of activated alumina.

^{1}H, $^{31}P\{^{1}H\}$, and 2D homo- and heteronuclear NMR experiments were performed on 400, 500, and 600 MHz spectrometers at 298 K. ^{1}H and 2D homonuclear (H−H) NMR spectra were referenced to residual NMR solvent peaks as appropriate, ^{31}P NMR spectra are reported relative to an 85% H_3PO_4 external standard (0 ppm), and 2D heteronuclear (C−H) spectra are referenced relative to TMS (0 ppm). κ^5-[(^{15c5}NCOP^{iPr})Ir(H)][BAr^F_4] (**1**),[7] κ^4-(^{15c5}NCOP^{iPr})Ir(H)(Cl) (**2**),[7] *cis*-κ^3-(^{15c5}NCOP^{iPr})Ir(H)(CO)(Cl) (**6-cis**),[8] *cis*-κ^3-(^{15c5}NCOP^{iPr})Ir(H)($NCCH_3$)(Cl) (**7-cis**),[7] κ^3-*trans*-(^{15c5}NCOP^{iPr})Ir-(H)(Cl)($NCCH_3$) (**7-trans**),[7] [κ^4-(^{15c5}NCOP^{iPr})Ir(H)($NCCH_3$)]-[BAr^F_4] (**11**),[7] [κ^3-(^{15c5}NCOP^{iPr})Ir(H)($NCCH_3$)$_2$][BAr^F_4] (**12**),[7] [κ^4-(^{15c5}NCOP^{iPr})Ir(H)(H_2O)][BAr^F_4] (**13**),[7] (^{15c5}NCOP^{iPr})(H),[7] PPNBr,[47] PPNI,[47] and $NaBAr^F_4$[48] were prepared according to literature procedures. All of the other reagents were commercially available and used without modification.

HRMS measurements (resolution 100 000, mass error ≤1 ppm) were performed with a Q Exactive Orbitrap mass spectrometer (ThermoFisher, Bremen, Germany). Samples were introduced via syringe pump into an atmospheric pressure photoionization source at a flow rate of 10 μL/min. Xcalibur (ThermoFisher, Breman, Germany) was used to analyze the data. Molecular formula assignments were determined with Molecular Formula Calculator (version 1.2.3).

Single-crystal X-ray diffraction data were collected on a Bruker APEX-II CCD diffractometer at 100 K with Cu Kα radiation (λ = 1.54175 Å). Structures were solved and refined using the Bruker SHELXTL[49,50] software package within Apex3[51] and/or OLEX2.[52] Further details are provided in the Supporting Information.

Synthesis of κ^4-(^{15c5}NCOP^{iPr})Ir(H)(Br) (3). In a 20 mL scintillation vial, 26.4 mg of **1** (39.5 μmol) and 23 mg of PPNBr (40.07 μmol) were dissolved in CH_2Cl_2 (5 mL), and the mixture was stirred for 2 h in a glovebox. The solvent was removed under vacuum, and the byproduct, [PPN][BAr^F_4], was removed with an ether wash (2 × 2 mL) to yield 14.3 mg (72% yield) of a yellow solid. The product was 92% pure according to multinuclear NMR spectroscopy (with 8% complex **2** present that carried over during the synthesis), so elemental analysis is not reported; this was sufficient purity for the present NMR studies. **^{1}H NMR** (500 MHz, $CDCl_3$): δ −31.23 (d, J = 25.9 Hz, 1H), Ir−*H*), 0.88 (dd, J = 15.6, 7.6 Hz, 3H, $CH(CH_3)_2$), 1.21 (m, 3H, $CH(CH_3)_2$), 1.37 (dd, J = 13.9, 6.9 Hz, 3H, $CH(CH_3)_2$), 1.45 (dd, J = 16.3, 7.2 Hz, 3H, $CH(CH_3)_2$), 2.36 (m, 1H, $CH(CH_3)_2$), 2.55 (m, 1H,

DOI: 10.1021/acs.inorgchem.7b01485
Inorg. Chem. 2017, 56, 11141−11150

$CH(CH_3)_2$), 3.01 (dd, J = 15.0, 2.5 Hz, 1H, crown-CH_2), 3.25 (dd, J = 15.7, 1.8 Hz, 1H, crown-CH_2), 3.33 (d, J = 11.4 Hz, 1H, crown-CH_2, 3.42−3.55 (m, 2H, crown-CH_2), 3.57−3.97 (m, 8H, crown-CH_2), 4.08−4.13 (m, 2H, crown-CH_2), 4.42 (m, 2H, ArCH_2N, 5.04 (t, J = 10.9 Hz, 1H, crown-CH_2), 5.10 (dd, J = 11.7, 11.5 Hz, 1H, crown-CH_2), 6.54 (d, J = 8.2 Hz, 1H, Ar−H,), 6.57 (d, J = 8.2 Hz, 1H, Ar−H), 6.71 (t, J = 7.5 Hz, 1H, Ar−H). **$^{13}C\{^1H\}$ NMR** (151 MHz, $CDCl_3$): δ 16.59 (d, J = 2.9 Hz). 17.41 (d, J = 3.0 Hz, $CH(CH_3)_2$)), 17.56 (s, $CH(CH_3)_2$) 17.95 (d, J = 6.6 Hz, $CH(CH_3)_2$)), 29.68 (d, J = 38.5 Hz, $CH(CH_3)_2$), 31.39 (d, J = 32.9 Hz, $CH(CH_3)_2$)), 63.51 (d, J = 2.7 Hz, crown-CH_2), 65.00 (d, J = 2.1 Hz, crown-CH_2), 67.54 (d, J = 2.5 Hz, crown-CH_2), 68.61 (s, crown-CH_2), 69.25 (s, crown-CH_2), 70.43 (s, crown-CH_2), 70.59 (s, crown-CH_2), 72.40 (d, J = 2.0 Hz, ArCH_2N), 72.95 (s, crown-CH_2), 73.22 (s, crown-CH_2), 76.19 (s, crown-CH_2), 107.32 (d, J = 11.5 Hz), 113.21 (s, C_{Ar}), 122.70 (s, C_{Ar}), 134.76 (s, C_{Ar}), 148.15 (d, J = 3.2 Hz, C_{Ar}), 162.81 (d, J = 3.4 Hz, C_{Ar}). **$^{31}P\{^1H\}$ NMR** (243 MHz, $CDCl_3$): δ 144.88. **HRMS**: (3^+−H, m/z 713.12744, calcd 713.127423).

Synthesis of κ^4-(^{15c5}NCOP^{iPr})Ir(H)(I) (4). In air, an NMR tube was charged with **2** (11.7 mg, 11.7 μmol), NaI (22.8 mg, 152 μmol), and $CDCl_3$. The mixture was heated overnight at 55 °C. Excess salt was filtered off, and the solvent was removed by rotary evaporation, yielding a yellow film (3.1 mg, 23% yield). **^{1}H NMR** (500 MHz, $CDCl_3$): δ −31.17 (d, J = 24.4 Hz, 1H, Ir−H), 0.90 (dd, J = 15.5, 6.9 Hz, 3H, $CH(CH_3)_2$), 1.25 (m, 3H, $CH(CH_3)_2$), 1.38 (dd, J = 14.2, 7.0 Hz, 3H, $CH(CH_3)_2$), 1.47 (dd, J = 16.2, 7.3 Hz, 3H, $CH(CH_3)_2$), 2.36 (m, 1H, $CH(CH_3)_2$), 2.58 (m, 1H, $CH(CH_3)_2$), 3.04 (d, J = 12.3 Hz, 1H, crown-CH_2), 3.25 (m, 2H, crown-CH_2), 3.45 (m, 1H, crown-CH_2), 3.54 (m, 2H, crown-CH_2), 3.62 (m, 2H, crown-CH_2), 3.72 (m, 3H, crown-CH_2), 3.86 (m, 4H, crown-CH_2), 4.04 (m, 1H, crown-CH_2), 4.14 (m, 1H, crown-CH_2), 4.29 (dd, J = 14.7, 12.8 Hz, 1H, crown-CH_2), 4.42 (m, 2H, ArCH_2N), 5.05 (t, J = 10.3 Hz, 1H, crown-CH_2), 5.31 (dd, J = 15.4, 12.1 Hz, 1H, crown-CH_2), 6.56 (d, J = 7.4 Hz, 1H, Ar−H), 6.60 (d, J = 7.8 Hz, 1H, Ar−H), 6.75 (t, J = 7.7 Hz, 1H, Ar−H). **$^{13}C\{^1H\}$ NMR** (126 MHz, $CDCl_3$): δ 17.10 (s, $C(CH_3)_2$), 17.64 (s, $C(CH_3)_2$), 18.22 (s, $C(CH_3)_2$), 19.21 (d, J = 5.4 Hz, $C(CH_3)_2$), 30.36 (d, J = 38.8 Hz, $C(CH_3)_2$), 31.25 (d, J = 33.6 Hz, $C(CH_3)_2$), 65.41 (d, J = 8.2 Hz, crown-CH_2), 68.11 (s, crown-CH_2), 68.65 (s, crown-CH_2), 69.37 (s, crown-CH_2), 70.54 (s, crown-CH_2), 70.63 (s, crown-CH_2), 72.11 (s, ArCH_2N), 72.99 (overlapping s, crown-CH_2), 76.42 (s, crown-CH_2), 107.49 (d, J = 11.7 Hz, C_{Ar}), 113.39 (s, C_{Ar}), 122.89 (s, C_{Ar}), 137.21 (s, C_{Ar}), 148.63 (s, C_{Ar}), 162.43 (s, C_{Ar}). **$^{31}P\{^1H\}$ NMR** (202 MHz, $CDCl_3$): δ 145.63. **HRMS:** (4^+−H, m/z 759.11467, calcd 759.11561). **Anal. Calcd** for $C_{40}H_{40}IIrNO_5P$: C, 36.32; H, 5.30; N, 1.84. Found: C, 35.14; H, 4.82; N, 1.75. Although the product was pure by NMR analysis and the expected mass was confirmed by HRMS, the analysis results suggest that a minor impurity (perhaps residual NaI) was present. No impact on the NMR analysis was expected.

Equilibrium Formation of κ^3-[(^{15c5}NCOP^{iPr})Ir(H)$(Cl)_2$]$^-$ (5). In air, complex **2** (21.60 mg, 23.3 μmol) was dissolved in $CDCl_3$. To this solution a stock solution of NBu_4Cl (89.7 mg, 322.8 μmol dissolved in 4 mL of $CDCl_3$) was added portionwise to the solution of **2**. An additional 20 equiv of NBu_4Cl (179.4 mg, 645.6 μmol) was added, with 44% conversion observed. Addition of over 150 equiv of NBu_4Cl drove the reaction forward to 99% conversion. Separation of **5** from excess chloride proved to be difficult; this species was not isolated.

Synthesis of *trans*-κ^3-(^{15c5}NCOP^{iPr})Ir(H)(Cl)(CO) (6-trans). In a Teflon-sealed 50 mL reaction vessel, **2** (34.9 mg, 52.2 μmol) was dissolved in CH_2Cl_2 (10 mL). The solution was freeze−pump−thaw degassed, and 1 atm CO was admitted to the reaction vessel at room temperature. Upon addition of CO, the yellow color faded, affording a clear, colorless solution. The solvent was removed by vacuum, yielding a white solid (23.8 mg, 66% yield). Single crystals suitable for X-ray diffraction were grown by layering pentanes over a concentrated solution of **6-trans** in toluene. ^{1}H NMR (600 MHz, $CDCl_3$): δ −7.02 (d, 23.8 Hz, 1H, Ir-H), 1.16−1.34 (m, 12H, $CH(CH_3)_2$), 2.45 (m, 1H, $CH(CH_3)_2$), 2.57 (m, 1H, $CH(CH_3)_2$), 3.28 (dt, J = 12.8, 5.90 Hz, 1H, crown-CH_2), 3.51 (m, 3H, crown-CH_2), 3.66 (m, 10H, crown-CH_2), 3.78 (m, 2H, crown-CH_2), 3.86 (dt, J = 10.8, 5.25 Hz, 1H, crown-CH_2), 4.01 (m, 2H, crown-CH_2), 4.20 (d, J = 13.1 Hz, 1H, ArCH_2N), 4.36 (m, 1H, crown-CH_2), 4.42 (dt, J = 14.4, 6.2 Hz, 1H, crown-CH_2), 4.60 (dd, J = 14.0, 3.4 Hz, 1H, ArCH_2N), 6.64 (d, J = 7.8 Hz, 1H, Ar−H), 6.73 (d, J = 7.8 Hz, 1H, Ar−H), 6.83 (t, J = 7.8 Hz, 1H, Ar−H). $^{13}C\{^1H\}$ NMR (151 MHz, $CDCl_3$): δ 16.42 (s, $CH(CH_3)_2$), 16.57 (s, $CH(CH_3)_2$), 17.35 (d, J = 3.4 Hz, $CH(CH_3)_2$), 17.63 (s, $CH(CH_3)_2$), 30.96 (d, J = 42.4 Hz, $CH(CH_3)_2$), 33.30 (d, J = 33.6 Hz, $CH(CH_3)_2$), 33.30 (s, crown-CH_2), 53.44 (s, crown-CH_2), 61.36 (d, J = 2.3 Hz, crown-CH_2), 62.86 (s, crown-CH_2), 66.56 (d, J = 2.1 Hz, crown-CH_2), 69.87 (s, crown-CH_2), 70.18 (s, crown-CH_2), 70.26 (s, crown-CH_2), 70.35 (s, crown-CH_2), 70.64 (s, crown-CH_2), 71.18 (s, crown-CH_2), 75.44 (d, J = 2.4 Hz, ArCH_2N), 108.58 (d, J = 11 Hz, C_{Ar}), 117.01 (s, C_{Ar}), 124.15 (s, C_{Ar}), 129.28 (d, J = 3.3 Hz, C_{Ar}), 143.42 (d, J = 2.4 Hz, C_{Ar}), 160.88 (C_{Ar}), 178.90 (dd, J = 56.6, 3.4 Hz, Ir−CO; note that the ^{1}H decoupler did not reach this downfield signal). **$^{31}P\{^1H\}$ NMR** (243 MHz, $CDCl_3$): δ 150.17. **IR** (toluene): ν(CO) 2017 cm^{-1}. **Anal. Calcd** for $C_{24}H_{40}ClIrNO_6P$: C, 41.34; H, 5.78; N, 2.01. Found: C, 41.08; H, 5.49; N, 1.91.

Synthesis of [κ^4-(^{15c5}NCOP^{iPr})Ir(H)(CO)][BAr$^F_4$] (8). A 20 mL scintillation vial was charged with (^{15c5}NCOP)Ir(H)(CO)(Cl) (0.0522 g, 0.0749 mmol), $NaBAr^F_4$ (0.0732 g, 0.0826 mmol), and CH_2Cl_2 (8 mL). The resulting yellow slurry was stirred for 17 h. The mixture was filtered, and the light-golden-yellow filtrate was concentrated to ∼1 mL under vacuum. Pentane (5 mL) was added, and the solvent was removed under vacuum, affording **8** as an off-white solid (0.0997 g, 87% yield). Single crystals suitable for X-ray diffraction were grown by slow evaporation of an Et_2O solution of **8** into $(Me_3Si)_2O$. **^{1}H NMR** (600 MHz, CD_2Cl_2): δ −25.67 (d, J = 21.4 Hz, 1H, Ir−H), 0.92 (dd, J = 16.8, 7.0 Hz, 3H, $CH(CH_3)_2$), 1.05 (dd, J = 20.9, 6.9 Hz, 3H, $CH(CH_3)_2$), 1.38 (dd, J = 18.9, 7.5 Hz, 3H, $CH(CH_3)_2$), 1.44 (dd, J = 14.8, 6.8 Hz, 3H, $CH(CH_3)_2$), 2.55 (overlapping m, 2H, $CH(CH_3)_2$), 3.06 (m, 1H, crown-CH_2), 3.58 (m, 9H, crown-CH_2), 3.78 (m, 4H, crown-CH_2), 3.93 (m, 1H, crown-CH_2), 4.01 (m, 2H, crown-CH_2), 4.18 (m, 1H, crown-CH_2), 4.28 (m, 2H, crown-CH_2), 4.58 (dd, J = 15.6, 2.9 Hz, 1H, ArCHHN), 4.63 (d, J = 15.7 Hz, 1H, ArCHHN), 6.80 (d, J = 7.7 Hz, 1H, Ar−H), 6.82 (d, J = 8.3 Hz, 1H, Ar−H), 7.07 (t, J = 7.8 Hz, 1H, Ar−H), 7.56 (s, 4H, p−B−Ar−H), 7.72 (s, 8H, o−B−Ar−H). **$^{13}C\{^1H\}$ NMR** (151 MHz, CD_2Cl_2): δ 16.12 (d, J = 4.7 Hz, $CH(CH_3)_2$), 17.37 (d, J = 2.3 Hz, $CH(CH_3)_2$), 17.86 (d, J = 4.0 Hz, $CH(CH_3)_2$), 18.20 (d, J = 6.3 Hz, $CH(CH_3)_2$), 29.69 (d, J = 38.9 Hz, $CH(CH_3)_2$), 31.93 (d, J = 36.0 Hz, $CH(CH_3)_2$), 66.13 (d, J = 1.4 Hz, crown-CH_2), 67.50 (s, crown-CH_2), 69.08 (s, crown-CH_2), 69.42 (d, J = 2.0 Hz, crown-CH_2), 70.52 (d, J = 2.4 Hz, crown-CH_2), 70.66 (s, crown-CH_2), 70.83 (s, crown-CH_2), 71.75 (s, crown-CH_2), 73.12 (s, crown-CH_2), 75.69 (d, J = 1.4 Hz, ArCH_2N), 78.56 (s, crown-CH_2), 110.16 (d, J = 12.3 Hz, C_{Ar}), 115.57 (s, C_{Ar}), 117.87 (p, J = 4.1 Hz, p-CH, BAr^F), 124.99 (q, J = 272.4 Hz, CF_3, BAr^F), 129.05 (s, C_{Ar}), 129.26 (qdd, J = 31.2, 5.8, 2.9 Hz, C−CF_3, BAr^F), 135.19 (s, o-CH, BAr^F), 145.87 (d, J = 5.0 Hz, C_{Ar}), 152.27 (d, J = 3.3 Hz, C_{Ar}), 162.14 (dd, J = 99.7, 49.9 Hz, B−C, BAr^F), 162.80 (d, J = 1.4 Hz, C_{Ar}), 183.35 (s, Ir−CO). **$^{31}P\{^1H\}$ NMR** (243 MHz, CD_2Cl_2): δ 152.77. **IR** (solid): ν(CO) 2041 cm^{-1}. **Anal. Calcd** for $C_{56}H_{52}BF_{24}IrNO_6P$: C, 44.11; H, 3.44; N, 0.92. Found: C, 44.38; H, 3.28; N, 0.95.

Synthesis of [κ^3-(^{15c5}NCOP^{iPr})Ir(H)$(CO)_2$][BAr$^F_4$] (9). A sample of **1** was dissolved in $CDCl_3$ and transferred to a Teflon-sealed NMR tube. The tube was freeze−pump−thaw degassed three times, and 1 atm CO was added at room temperature. After 30 min, an equilibrium mixture of **8** and **9** was apparent by NMR spectroscopy. Backfilling again with CO saw further conversion to 87%. Complex **9** is stable only under a CO atmosphere, so this product was not isolated. **^{1}H NMR** (600 MHz, $CDCl_3$): δ −9.42 (d, J = 20.8 Hz, 1H, Ir−H), 1.07−1.14 (m, 6H, $CH(CH_3)_2$), 1.15−1.26 (m, 6H, $CH(CH_3)_2$), 2.52 (m, 2H, $CH(CH_3)_2$, 3.56−3.82 (m, 14H, crown-CH_2), 3.83−3.92 (m, 2H, crown-CH_2), 4.03 (m, 1H, crown-CH_2), 4.21 (m, 1H, crown-CH_2), 4.46 (d, J = 14.7 Hz, 1H, ArCH_2N), 4.59 (dd, J = 14.7, 3.43 Hz, 1H, ArCH_2N), 6.85 (d, J = 8.2 Hz, 1H, Ar−H) 6.99 (d, J = 7.0 Hz, 1H, Ar−H), 7.08 (m, 1H, Ar−H). **$^{13}C\{^1H\}$ NMR** (151 MHz, $CDCl_3$): δ 16.45 (s, 3H, $CH(CH_3)_2$), 16.61 (s, 3H, $CH(CH_3)_2$), 17.29 (d, J = 2.6 Hz, 3H, $CH(CH_3)_2$), 17.43 (d, J = 3.4 Hz, 3H, $CH(CH_3)_2$), 30.64 (d, J = 42.1 Hz, 1H, $CH(CH_3)_2$), 33.88 (d, J = 34.8 Hz, 1H, $CH(CH_3)_2$),

DOI: 10.1021/acs.inorgchem.7b01485
Inorg. Chem. 2017, 56, 11141−11150

67.14 (s, crown-CH_2), 67.55 (s, crown-CH_2), 67.71 (s, crown-CH_2), 69.76 (s, crown-CH_2), 69.89 (s, crown-CH_2), 70.07 (s, crown-CH_2), 70.27 (s, crown-CH_2), 70.48 (s, crown-CH_2), 70.48 (s, crown-CH_2), 70.55 (s, crown-CH_2), 70.95 (s, $ArCH_2N$), 111.02 (d, J = 12.3 Hz, C_{Ar}), 117.44 (p, J = 11.7 Hz, p-CH, BAr^F), 119.3 (s, C_{Ar}), 124.52 (q, J = 272.5 Hz, BAr^F), 128.7 (s, C_{Ar}), 128.76 (qdd, J = 31.5, 5.9, 2.9 Hz, $C-CF_3$, BAr^F), 129.87 (d, J = 4.0 Hz, C_{Ar}), 134.76 (s, o-CH, BAr^F), 145.37 (d, J = 2.0 Hz, C_{Ar}), 161.13 (s, C_{Ar}), 161.54 (dd, J = 100.7, 48.67 Hz, *ipso*-C, BAr^F), 168.51 (d, J = 2.9 Hz, *trans*-CO), 169.81 (s, *cis*-CO). **$^{31}P\{^1H\}$ NMR** (243 MHz, $CDCl_3$): δ 170.62. **IR** (CH_2Cl_2): ν(CO) 2099, 2062 cm^{-1}.

Decarbonylation of 6-cis. A 20 mL scintillation vial charged with compound **6-cis** (9.6 mg, 6.3 μmol), trimethylamine *N*-oxide (5 mg, 66.6 μmol), and THF was allowed to stir overnight. The solvent was removed under vacuum, and the crude reaction mixture was taken up in C_6D_6 for NMR analysis.

■ ASSOCIATED CONTENT

Supporting Information

The Supporting Information is available free of charge on the ACS Publications website at DOI: 10.1021/acs.inorgchem.7b01485.

NMR characterization, methodology for determination of $\Delta\delta$ values, and X-ray crystallographic details (PDF)

Accession Codes

CCDC 1535958 and 1555314 contain the supplementary crystallographic data for this paper. These data can be obtained free of charge via www.ccdc.cam.ac.uk/data_request/cif, or by e-mailing data_request@ccdc.cam.ac.uk, or by contacting The Cambridge Crystallographic Data Centre, 12 Union Road, Cambridge CB2 1EZ, U.K.; fax: +44 1223 336033.

■ AUTHOR INFORMATION

Corresponding Author

*E-mail: ajmm@email.unc.edu.

ORCID

Diane A. Dickie: 0000-0003-0939-3309

Alexander J. M. Miller: 0000-0001-9390-3951

Notes

The authors declare no competing financial interest.

■ ACKNOWLEDGMENTS

This material is based upon work supported by the National Science Foundation (NSF) under CHE-1553802. J.G. was supported by an NSF Graduate Research Fellowship (DGE-1144081). A.J.M.M. is an Alfred P. Sloan Fellow. We thank Marc ter Horst for assisting with NMR spectroscopy, Quinton Bruch for assisting with X-ray crystallography, and Brandie Ehrmann of the University of North Carolina's Department of Chemistry Mass Spectrometry Core Laboratory for assistance with mass spectroscopy.

■ REFERENCES

(1) Jeffrey, J. C.; Rauchfuss, T. B. Metal Complexes of Hemilabile Ligands. Reactivity and Structure of Dichlorobis(o-(diphenylphosphino)anisole)ruthenium(II). *Inorg. Chem.* **1979**, *18*, 2658−2666.

(2) Bader, A.; Lindner, E. Coordination Chemistry and Catalysis with Hemilabile Oxygen-Phosphorus Ligands. *Coord. Chem. Rev.* **1991**, *108*, 27−110.

(3) Kwong, F.; Chan, A. Recent Developments on Hemilabile P,O-Type Ligands in Cross-Coupling Reactions. *Synlett* **2008**, 1440−1448.

(4) Mark, S.; Wadepohl, H.; Enders, M. Molecular Weight Control in Organochromium Olefin Polymerization Catalysis by Hemilabile Ligand-Metal Interactions. *Beilstein J. Org. Chem.* **2016**, *12*, 1372−1379.

(5) Kingsbury, J. S.; Harrity, J. P. A.; Bonitatebus, P. J.; Hoveyda, A. H. A Recyclable Ru-Based Metathesis Catalyst. *J. Am. Chem. Soc.* **1999**, *121*, 791−799.

(6) Matsugi, M.; Curran, D. P. Synthesis, Reaction, and Recycle of Light Fluorous Grubbs-Hoveyda Catalysts for Alkene Metathesis. *J. Org. Chem.* **2005**, *70*, 1636−1642.

(7) Kita, M. R.; Miller, A. J. M. Cation-Modulated Reactivity of Iridium Hydride Pincer-Crown Ether Complexes. *J. Am. Chem. Soc.* **2014**, *136*, 14519−14529.

(8) Grajeda, J.; Kita, M. R.; Gregor, L. C.; White, P. S.; Miller, A. J. M. Diverse Cation-Promoted Reactivity of Iridium Carbonyl Pincer-Crown Ether Complexes. *Organometallics* **2016**, *35*, 306−316.

(9) Gregor, L. C.; Grajeda, J.; Kita, M. R.; White, P. S.; Vetter, A. J.; Miller, A. J. M. Modulating the Elementary Steps of Methanol Carbonylation by Bridging the Primary and Secondary Coordination Spheres. *Organometallics* **2016**, *35*, 3074−3086.

(10) Miller, A. J. M. Cation-Modulated Hemilability in Pincer-Crown Ether Ligands: A Strategy for Tunable and Switchable Catalysis. *Dalton Trans.* **2017**, DOI: 10.1039/C7DT02156A.

(11) Slone, C. S.; Weinberger, D. A.; Mirkin, C. A. The Transition Metal Coordination Chemistry of Hemilabile Ligands. *Prog. Inorg. Chem.* **1999**, *48*, 233−350.

(12) Machan, C. W.; Lifschitz, A. M.; Stern, C. L.; Sarjeant, A. A.; Mirkin, C. A. Crystallographic Snapshots of the Bond-Breaking Isomerization Reactions Involving Nickel(II) Complexes with Hemilabile Ligands. *Angew. Chem., Int. Ed.* **2012**, *51*, 1469−1472.

(13) Baranac-Stojanović, M. New Insight into the Anisotropic Effects in Solution-State NMR Spectroscopy. *RSC Adv.* **2014**, *4*, 308−321.

(14) Otting, G. Protein NMR Using Paramagnetic Ions. *Annu. Rev. Biophys.* **2010**, *39*, 387−405.

(15) Pascal, R. A.; Grossman, R. B.; Van Engen, D. Synthesis of in-[34,10][7]metacyclophane: Projection of an Aliphatic Hydrogen toward the Center of an Aromatic Ring. *J. Am. Chem. Soc.* **1987**, *109*, 6878−6880.

(16) Karabatsos, G. J.; Sonnichsen, G. C.; Hsi, N.; Fenoglio, D. J. Structure by Nuclear Magnetic Resonance. XIV. Anisotropic Effects of the Carbonyl Group. *J. Am. Chem. Soc.* **1967**, *89*, 5067−5068.

(17) Cross, A. D.; Harrison, I. T. Spectra and Stereochemistry. VII. Long-Range Shielding by Nitrile Groups. *J. Am. Chem. Soc.* **1963**, *85*, 3223−3228.

(18) Prestegard, J. H. New Techniques in Structural NMR — Anisotropic Interactions. *Nat. Struct. Biol.* **1998**, *5*, 517−522.

(19) Liu, Y.; Saurí, J.; Mevers, E.; Peczuh, M. W.; Hiemstra, H.; Clardy, J.; Martin, G. E.; Williamson, R. T. Unequivocal Determination of Complex Molecular Structures Using Anisotropic NMR Measurements. *Science* **2017**, *356*, eaam5349.

(20) Hua, X.; von Zelewsky, A. Enantiomerically Pure Chiral Ru^{II}(L-L)$_2$ Building Blocks for Coordination Compounds. *Inorg. Chem.* **1995**, *34*, 5791−5797.

(21) Cotton, F. A.; Kitagawa, S. Preparation, Spectroscopic Properties, and Characterization of *anti*- and *syn*-α-$Mo_2Cl_4[(C_6H_5)_2PCH_2CH_2P(p\text{-}CH_3C_6H_4)_2]$ in Solution and in the Solid State. *Inorg. Chem.* **1987**, *26*, 3463−3468.

(22) McGlinchey, M. J. 2000 Alcan Award Lecture Adventures in Organometallic NMR: Steric Restraints, Slowed Rotations, and Skeletal Rearrangements. *Can. J. Chem.* **2001**, *79*, 1295−1309.

(23) Mitchell, R. H.; Brkic, Z.; Berg, D. J.; Barclay, T. M. Effective Aromaticity of Tricarbonylchromiumbenzene, about 25% Enhanced over that of Benzene: Structural Evidence from a Complexed Benzannulene. *J. Am. Chem. Soc.* **2002**, *124*, 11983−11988.

(24) Appleton, T. G.; Clark, H. C.; Manzer, L. E. The Trans-Influence: Its Measurement and Significance. *Coord. Chem. Rev.* **1973**, *10*, 335−422.

(25) Babbini, D. C.; Iluc, V. M. Iridium $PC_{sp3}P$-Type Complexes with a Hemilabile Anisole Tether. *Organometallics* **2015**, *34*, 3141−3151.

DOI: 10.1021/acs.inorgchem.7b01485
Inorg. Chem. 2017, 56, 11141−11150

(26) Kita, M. R.; Miller, A. J. M. An Ion-Responsive Pincer−Crown Ether Catalyst System for Rapid and Switchable Olefin Isomerization. *Angew. Chem., Int. Ed.* **2017**, *56*, 5498−5502.
(27) Rybtchinski, B.; Ben-David, Y.; Milstein, D. Unexpected Isomerization of a *Cis* - into a *Trans* - Dihydride Complex. A Neutral Late Transition Metal Complex as a Hydride Donor. *Organometallics* **1997**, *16*, 3786−3793.
(28) Goldberg, J. M.; Wong, G. W.; Brastow, K. E.; Kaminsky, W.; Goldberg, K. I.; Heinekey, D. M. The Importance of Steric Factors in Iridium Pincer Complexes. *Organometallics* **2015**, *34*, 753−762.
(29) Adams, J. J.; Arulsamy, N.; Roddick, D. M. Acceptor PCP Pincer Iridium(I) Chemistry: Stabilization of Nonmeridional PCP Coordination Geometries. *Organometallics* **2011**, *30*, 697−711.
(30) Luh, T.-Y. Trimethylamine N-Oxide-A Versatile Reagent For Organometallic Chemistry. *Coord. Chem. Rev.* **1984**, *60*, 255−276.
(31) Semenov, V. A.; Samultsev, D. O.; Krivdin, L. B. Theoretical and Experimental Study of 15 N NMR Protonation Shifts. *Magn. Reson. Chem.* **2015**, *53*, 433−441.
(32) Iglesias, M.; Pérez-Nicolás, M.; Miguel, P. J. S.; Polo, V.; Fernández-Alvarez, F. J.; Pérez-Torrente, J. J.; Oro, L. A. A Synthon for a 14-Electron Ir(III) Species: Catalyst for Highly Selective β-(Z) Hydrosilylation of Terminal Alkynes. *Chem. Commun.* **2012**, *48*, 9480−9482.
(33) Iguchi, K.; Kaneta, S.; Mori, K.; Yamada, Y.; Honda, A.; Mori, Y. Bromovulone I and Iodovulone I, Unprecedented Brominated and Iodinated Marine Prostanoids with Anittumour Activity Isolated from the Japanese Stolonifer *Clavularis viridis* Quoy and Galmard. *J. Chem. Soc., Chem. Commun.* **1986**, 981−982.
(34) Kleinpeter, E.; Koch, A.; Seidl, P. R. Visualization and Quantification of the Anisotropic Effect of C═C Double Bonds on ^{1}H NMR Spectra of Highly Congested Hydrocarbons-Indirect Estimates of Steric Strain. *J. Phys. Chem. A* **2008**, *112*, 4989−4995.
(35) Winstein, S.; Carter, P.; Anet, F. A. L.; Bourn, A. J. R. The Effects of Steric Compression on Chemical Shifts in Half-Cage and Related Molecules. *J. Am. Chem. Soc.* **1965**, *87*, 5247−5249.
(36) Kleinpeter, E.; Klod, S. Separation of Anisotropic and Steric Substituent Effects - Nuclear Chemical Shielding Analysis of H-4 and C-4 in Phenanthrene and 11-Ethynylphenanthrene. *J. Am. Chem. Soc.* **2004**, *126*, 2231−2236.
(37) Afonin, A. V. Effect of Aromatic Ring Anisotropy on the ^{1}H NMR Shielding Constants and Conformational Equilibrium of Sterically Strained Aryl Vinyl Ethers. *Russ. J. Org. Chem.* **2011**, *47*, 496−499.
(38) Tori, K.; Aono, K.; Kitahonoki, K.; Takano, Y.; Muneyuki, R.; Tanida, H.; Tsuji, T. NMR Studies of Bridged Ring Systems. X. Long-Range Anisotropic Shielding Effects of an Epoxide and an Azridine Ring. *Tetrahedron Lett.* **1966**, *7*, 2921−2926.
(39) Kleinpeter, E.; Stoss, S.; Gabler, M.; Schroth, W. The Stereochemistry of Crown Ethers. *Magn. Reson. Chem.* **1989**, *27*, 676−683.
(40) Vougioukalakis, G. C.; Grubbs, H. Ruthenium-Based Heterocyclic Carbene-Coordinated Olefin Metathesis Catalysts. *Chem. Rev.* **2010**, *110*, 1756−1787.
(41) Weng, Z.; Teo, S.; Hor, T. S. A. Metal Unsaturation and Ligand Hemilability in Suzuki Coupling. *Acc. Chem. Res.* **2007**, *40*, 676−684.
(42) Ryken, S. A.; Schafer, L. L. N,O-Chelating Four-Membered Metallacyclic Titanium(IV) Complexes for Atom-Economic Catalytic Reactions. *Acc. Chem. Res.* **2015**, *48*, 2576−2586.
(43) Bei, X.; Uno, T.; Norris, J.; Turner, H. W.; Weinberg, W. H.; Guram, A. S.; Petersen, J. L. Phenyl Backbone-Derived P, O- and P, N-Ligands for Palladium/Ligand-Catalyzed Aminations of Aryl Bromides, Iodides, and Chlorides. Syntheses and Structures of (P, O)$_n$-Palladium(II)Aryl(Br) Complexes. *Organometallics* **1999**, *18*, 1840−1853.
(44) Lindner, E.; Scheytt, C.; Wegner, P. Neuartige Basische Liganden Fur Die Homogenkatalytische Methanolcarbonylierung. *J. Organomet. Chem.* **1986**, *308*, 311−323.
(45) Jung, S.; Brandt, C. D.; Werner, H. A Cationic Allenylideneruthenium(II) Complex with Two Bulky Hemilabile Phosphine Ligands. *New J. Chem.* **2001**, *25*, 1101−1103.
(46) Liu, Y.; Kean, Z. S.; d'Aquino, A. I.; Manraj, Y. D.; Mendez-arroyo, J.; Mirkin, C. A. Palladium(II) Weak-Link Approach Complexes Bearing Hemilabile N-Heterocyclic Carbene−Thioether Ligands. *Inorg. Chem.* **2017**, *56*, 5902−5910.
(47) Martinsen, A.; Songstad, J.; Larsson, R.; Pouchard, M.; Hagenmuller, P.; Andresen, A. F. Preparation and Properties of Some Bis(triphenylphosphine)iminium Salts, $[(Ph_3P)_2N]X$. *Acta Chem. Scand.* **1977**, *31a*, 645−650.
(48) Yakelis, N. A.; Bergman, R. G. Safe Preparation and Purification of Sodium Tetrakis[(3,5-trifluoromethyl)phenyl]borate ($NaBAr^F_{24}$): Reliable and Sensitive Analysis of Water in Solutions of Fluorinated Tetraarylborates. *Organometallics* **2005**, *24*, 3579−3581.
(49) Sheldrick, G. M. Crystal Structure Refinement with SHELXL. *Acta Crystallogr., Sect. C: Struct. Chem.* **2015**, *71*, 3−8.
(50) Sheldrick, G. M. A Short History of SHELX. *Acta Crystallogr., Sect. A: Found. Crystallogr.* **2008**, *64*, 112−122.
(51) *Saint; SADABS; Apex3*; Bruker AXS: Madison, WI, 2012.
(52) Dolomanov, O. V.; Bourhis, L. J.; Gildea, R. J.; Howard, J. A. K.; Puschmann, H. OLEX2: A Complete Structure Solution, Refinement and Analysis Program. *J. Appl. Crystallogr.* **2009**, *42*, 339−341.

DOI: 10.1021/acs.inorgchem.7b01485
Inorg. Chem. 2017, 56, 11141−11150